Progress In Electromagnetics Research M, Vol. 108, 27–38, 2022

Ultra-Wideband CPW Fed Band-Notched Monopole Antenna Optimization Using Machine Learning

Pinku Ranjan[1], Ankit Maurya[1], Harshit Gupta[1], Swati Yadav[2], and Anand Sharma[3, *]

Abstract—In this article, a compact Coplanar Waveguide (CPW) fed band-notched monopole antenna is designed and optimized. The unique feature of this article is to provide an approach for designing an antenna in the best way using machine learning techniques. Machine Learning can be used to speed up the antenna design process. There are five algorithms employed: Decision Tree, Random Forest, XGBoost Regression, K-Nearest Neighbor (KNN), and Artificial Neural Network (ANN). Among all the algorithms, KNN gives the best result with accuracy up to 98%. From the obtained result, we can estimate the dimensions of the desired parameters, which could not be done previously by High Frequency Structure Simulator (HFSS) Electromagnetic (EM) simulator. The optimized antenna design is also fabricated and tested, which confirms its frequency range between 2.9 and 21.6 GHz. Stable radiation features in between the operating frequency range makes it suitable for Ultra-Wideband (UWB) applications.

1. INTRODUCTION

In recent years, the demand for high-speed and reliable communication networks is continuously increasing. **Ultra-wideband** (UWB) antennas are one of the possible solutions for achieving it. The Federal Communications Commission (FCC) has allocated the frequency band from 3.1 to 10.6 GHz for unlicensed UWB services [1]. **Electromagnetic** (EM) simulators such as **High Frequency Structure Simulator** (HFSS) are widely used for the design and optimization of antennas. The optimization will be carried out by changing the size of different parameters of the antenna to meet the desired parameters. Traditionally, the optimization process is carried out by means of test and error method. This is because the optimization process takes time. From the last one decade, as the cost of storing and processing data has dropped dramatically, machine learning has been increasingly used in various fields. It is very easy to use machine learning for finding out the optimized solutions. Machine learning approaches can be used to create multiple antenna models in order to provide accurate and quick design parameter predictions. It will find the hidden mathematical relationships in the data, allowing us to link input and output behaviors and create predictions.

In previous years, many UWB antennas for wireless application have been designed [2–7]. Due to the wide frequency range of UWB antennas, the major disadvantage with UWB systems is its interference with the other existing systems. Therefore, to avoid the interference with the other wireless systems it is necessary to notch out portions of the band. Various methods are used to develop the band notched characteristic in UWB antennas [8–13]. In previous years, many band notched antennas were designed using various techniques. But, all the previously available antennas are big in size with small

Received 28 December 2021, Accepted 17 January 2022, Scheduled 8 February 2022
* Corresponding author: Anand Sharma (anandsharma@mnnit.ac.in).
[1] Atal Bihari Vajpayee — Indian Institute of Information Technology & Management, Gwalior, India. [2] Department of Electronics and Telecommunication Engineering, College of Engineering Roorkee, Roorkee, India. [3] Department of Electronics and Communication Engineering, Motilal Nehru National Institute of Technology Allahabad, Prayagraj, India.

bandwidth. Therefore the need for an antenna with a large ultra-wide bandwidth and band-notched characteristics increases.

In this paper, a compact CPW-fed UWB antenna with an inverted U-shaped radiator and two rectangular ground planes is proposed. Tapered microstrip feed line is used to excite the antenna. The proposed UWB antenna works in the frequency range from 2.9 to 21.6 GHz. Further, to minimize the interference at Worldwide Interoperability for Microwave Access (WiMAX) band, the frequency range from 3.3 to 3.8 GHz is rejected with the assistance of an inverted L-shape slot. Table 1 shows the comparison of the previously available band notched antennas with the proposed one.

Table 1. Comparison of various band-notched UWB antennas with proposed antenna.

Ref. #	Size (mm^3)	Bands Covered (GHz)	Notched Band (GHz)
[16]	$30 \times 28 \times 0.8$ 3.0	3.0–11	5.0–5.8
[17, 18]	$34 \times 27 \times 0.5$	3.0–11	3.3–3.8 and 5.1–5.8
[19]	$22.5 \times 22.5 \times 1$	3.1–10.6	4.1–5.8
[20]	$24 \times 34.6 \times 0.8$	3.1–10.6	3.4–3.8 and 5.4–5.8
[21]	$30 \times 31 \times 1.5$	3.1–10.6	5.0–6.0
Proposed Antenna	$23 \times 10 \times 0.8$	2.9–21.6	3.2–3.9

In this article, machine learning is typically defined as a way for programming computers to maximise a performance criterion by examining historical samples. Models are typically built using data gathered from specific examples. Artificial neural networks, support vector regression, genetic algorithms, evolution computing, and other machine-learning approaches are included in this context [14, 15]. Machine learning (ML) technology is used for antenna design optimization. Using machine learning algorithms, it is hoped that the reflection coefficient (S_{11}) can be predicted based on antenna parameters. Thus, it can help us avoid the endless loop of optimization through trial and error. There are five algorithms used in this research: Decision Tree, Random Forest, XGBoost Regression, K-Nearest Neighbor (KNN), and Artificial Neural Network (ANN). These algorithms were chosen because they can compute regression for nonlinear data, since the dataset generated after simulation is nonlinear. In conducting this research, a dataset consisting of resonance frequency, length, width, and thickness of the L-shaped slot is obtained after antenna simulation using HFSS. Then, different ML algorithms are used to predict the values. The R-square score value and Mean Squared Error (MSE) value for the simulated and predicted reflectance coefficients (S_{11}) are analyzed to measure the prediction accuracy.

2. METHODOLOGY

2.1. Antenna Design and Configurations

The top view of the proposed UWB antenna with all the parametric values is shown in Fig. 1. The antenna is fabricated on an FR-4 substrate. The thickness of the substrate is 0.8 mm with dielectric constant $\varepsilon_r = 4.4$ and loss tangent $\tan\delta = 0.02$. To design the antenna, an inverted U-shaped patch is used as the radiator, and two rectangular ground planes are designed on the two sides of the feed line. The inverted U-shaped radiator is connected to the ground plane using an arc shape structure. Also, for the good impedance matching in the operational bandwidth, two small slots are etched from the ground plane. The length and width of the slot are 2.2 mm and 0.35 mm, respectively. Further, an inverted L-shaped slot is etched from the radiator to get the band-notched characteristic at the WiMAX (3.3–3.7 GHz) band. The antenna has a circular shape from the top with a radius of 4 mm.

The simulated S-parameter curve for the presented antenna structure is shown in Fig. 2. From Fig. 2, it is clear that the antenna possesses the bandwidth of 18.7 GHz (from 2.9–21.6 GHz) together with the band-notch characteristic at WiMAX band range from 3.2 to 3.9 GHz. To study the effect of the length and width of L-shaped slots on the frequency range of the notched antenna, the band length (h), width (l), and thickness (d) are varied. First, the length is varied from 3 mm to 7 mm. Simulated

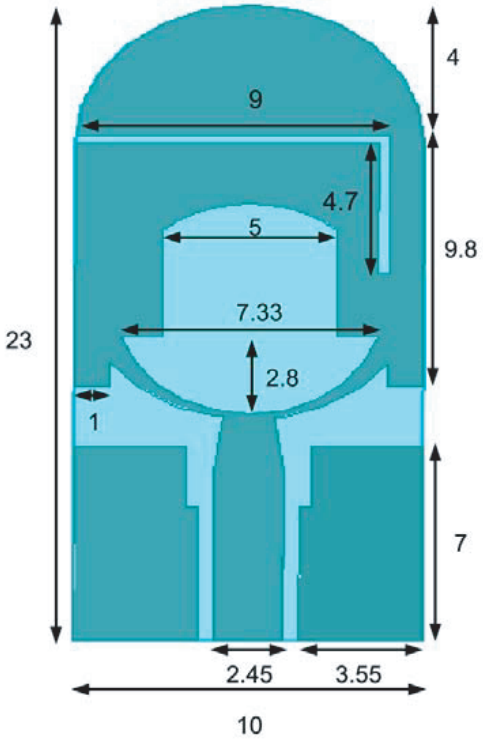

Figure 1. Geometry of the proposed CPW-fed band-notched UWB antenna.

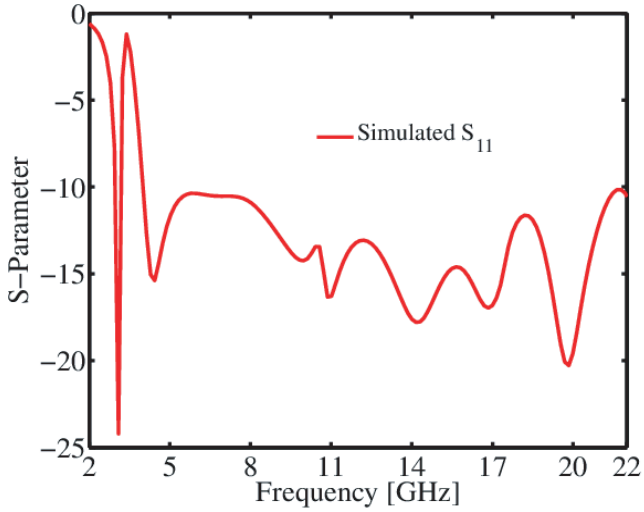

Figure 2. Simulated S-parameter of the proposed antenna.

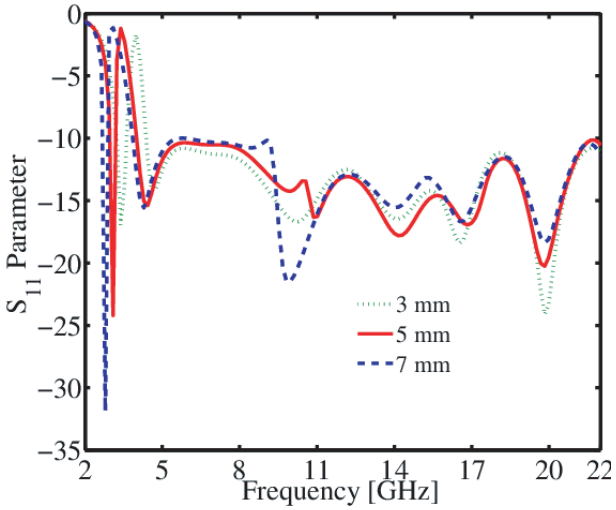

Figure 3. Variation for the length of the inverted L-shaped slot.

S-parameter curve of the proposed antenna for different lengths of L-shaped slot is depicted in Fig. 3. From Fig. 3, it can be seen that as the length of slot increases, the notched band is shifted towards the lower frequency range. The length of the current path at the resonant frequency would be half of the guided wavelength. Therefore,

$$L_1 = length\ (h) + width\ (l) - Thickness\ of\ slot\ (d)$$

The L-shaped slot acts as a quarter-guided wavelength resonator, and thus a center rejected frequency

f_n may be empirically approximated by [21]

$$f_n = \frac{C}{4L_1\sqrt{\frac{\varepsilon_r + 1}{2}}} \tag{1}$$

where L_1 is the overall slot length; h and l are the length and width of the L-shaped slot; ε_r is the relative dielectric constant; and c is the speed of the light. The total length calculated for the L-shaped slot is 13.7 mm for the center frequency of band-notched at 3.33 GHz. The design method is further validated by predicting the notch frequency for the data presented in Fig. 3 and Table 2, and the notched resonant frequency as a function of L_1 is compared with the full-wave simulated data.

Table 2. Comparison of notched design equation and full-wave simulated data.

h (mm)	L_1 (mm)	Resonant Frequency (GHz)	
		Full-wave simulation	Design equation
3	11.7	3.89	3.9
5	13.7	3.35	3.33
7	15.7	2.8	2.90

From Fig. 3, it is clear that the resonant frequencies calculated from the design method are in agreement with the simulated data. Therefore, to get the band-notched characteristic at the WiMAX band, 5 mm is selected as the final value for the length of the L-shaped slot.

The variation of the width of the L-shaped slot (for 3 values) is shown in Fig. 4. As seen from Fig. 4, with increasing the width of the slot, the band is shifted towards the lower frequency range. The bandwidth is also changed by varying the slot width. Therefore, to get the desired band-notched characteristic, 9.0 mm is chosen as the final value.

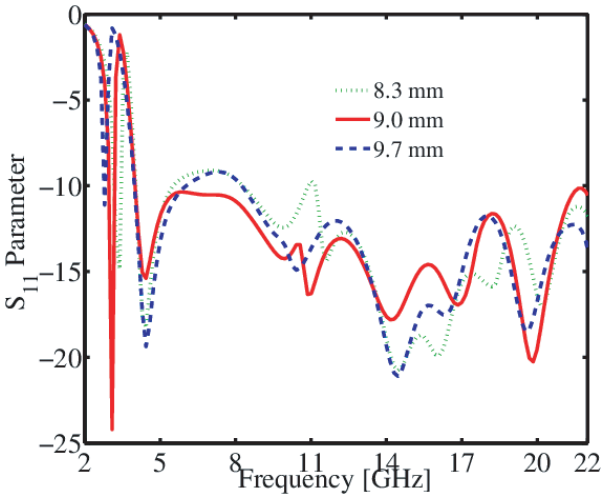

Figure 4. Variation for the width of the inverted L-shaped slot.

Figure 5(a) shows the surface current density at 3.3 GHz. At this frequency, the current is mainly concentrated around the L-shaped slot, which confirms the notch operation at this frequency band. Fig. 5(b) and Fig. 5(c) show the surface current densities at 7.5 GHz and 18.7 GHz, respectively. It is clearly observed from Fig. 5(b) that the current is mainly distributed on the two ground planes and the feed line. From Fig. 5(c), it is observed that the current is distributed in the lower part of the radiator and the upper part of the rectangular ground.

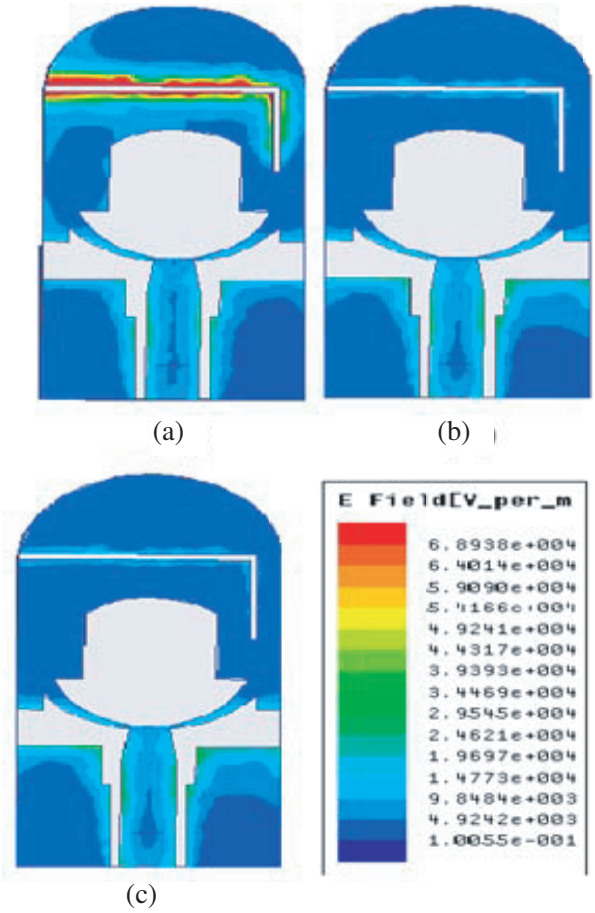

Figure 5. Surface current densities for band-notched UWB antenna at (a) 3.3 GHz, (b) 7.5 GHz, and (c) 18.7 GHz.

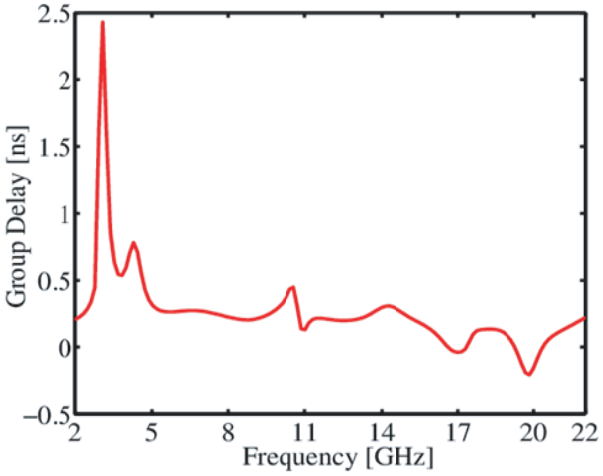

Figure 6. Group delay for the proposed antenna.

The time domain analysis of the proposed antenna is done using the group delay of the antenna. Pulses distortion of the antenna signal is measured using the group delay as shown in Fig. 6. The value of group delay should be constant to have the minimum pulse distortion and linear phase response.

From Fig. 6, it is observed that the variation of group delay is lower than 1 ns for the UWB, and at the notched band the variation exceeds 1 ns. The graph of group delay shows the linear phase response for the entire UWB and pulse distortion at the notched band.

3. DATASET

To obtain a dataset, the proposed antenna is designed over HFSS EM simulator. This dataset will be used to make predictions. Two parameters are observed in the simulation of the antenna. The 1st one is the resonant frequency (Freq), and 2nd one is the return loss or reflection coefficient (S_{11}).

After running simulations on HFSS, the simulation results are collected and stored. The dataset (which we got after simulating the antenna) consists of 201 records and is divided into 1009 features.

Dataset is collected with varying the length (h), width (l), and thickness (d) of L-shaped slots. After this, a new dataset is prepared. The new dataset consists of 202608 records and is divided into 5 features: the resonant frequency (Freq), horizontal length (h), vertical length (d), width of L-shaped slots (d), and return loss (dB) at the resonant frequency. The first four features are used as independent variables, while the last one is used as dependent variables.

Figure 7 shows the relationship between dependent and independent variables using some plots. For predicting the best parameters using the ML algorithm, the range of values is selected for different

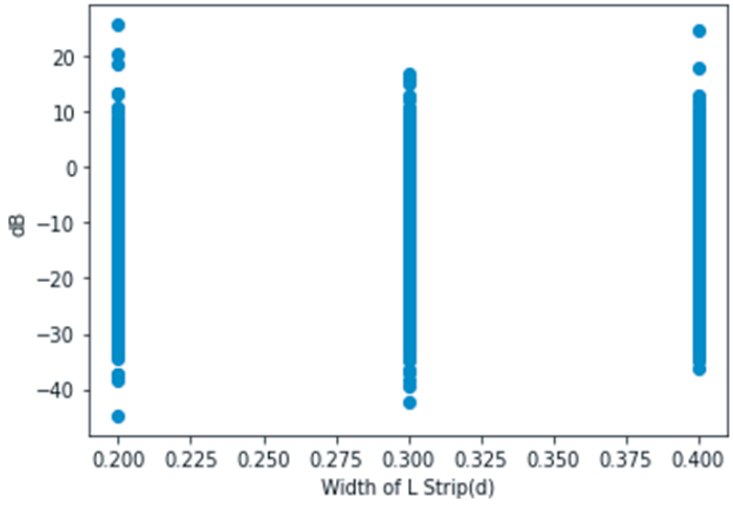

(a)

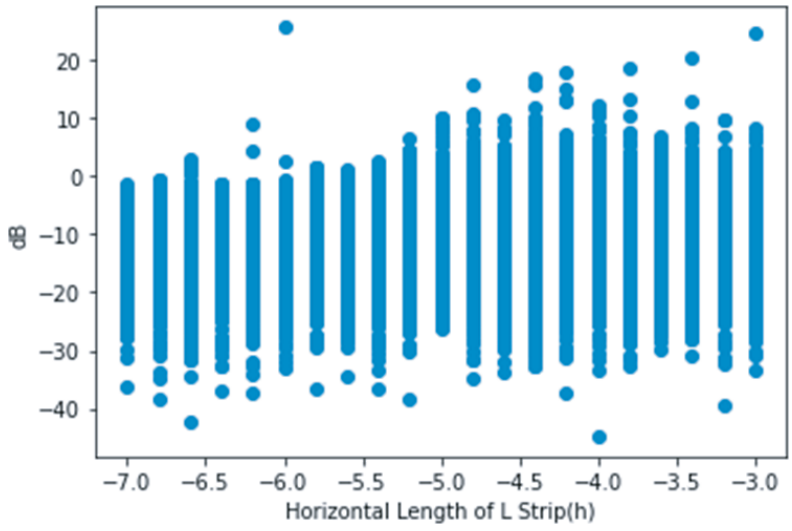

(b)

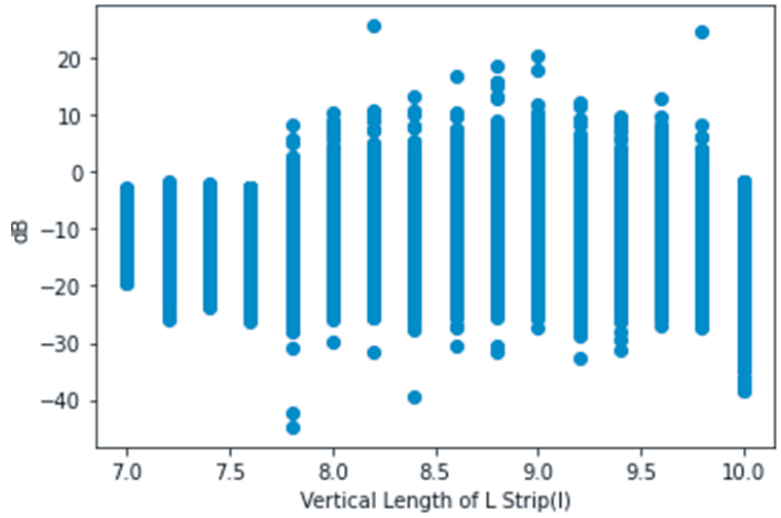

(c)

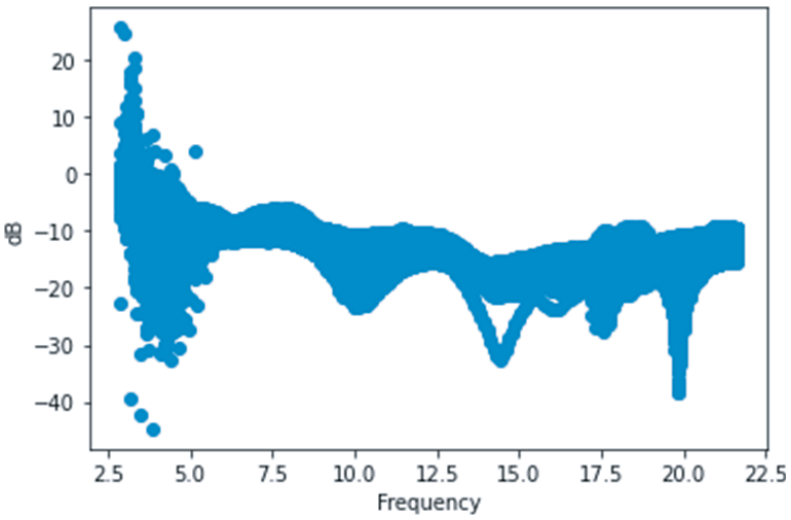

(d)

Figure 7. (a) Depicting the relationship between the width of L strip and return loss. (b) Depicting the relationship between the horizontal length of L strip and return loss. (c) Depicting the relationship between the vertical length of L strip and return loss. (d) Depicting the relationship between the resonant frequency and return loss.

parameters. Width of the L strip is varied from 0.2 to 0.5 mm with a difference of 0.1 mm, which gives us 3 different values for this parameter. Similarly, horizontal length of the L strip is varied from −3 to −7.1 mm with the difference −0.1 mm, which gives us 41 different values. Similarly, vertical length of L strip is varied from 7 to 10.1 mm with the difference 0.1 mm, which gives us 31 different values. Earlier, we had 201 values for the frequency between 2.9 and 21.6 GHz. So, after combining all values of these 4 parameters, a dataset of 766,413 rows and 4 columns is created.

After training the ML models with the dataset obtained from HFSS, the best model is selected on the basis of the highest R-square score and lowest MSE value. Then, this dataset is run on that model and will predict the S_{11} value for it. Then, we will select those parameters, which give us the lowest S_{11} value.

4. MACHINE LEARNING ALGORITHM AND IMPLEMENTATION

Machine learning has swept the world with its frequent applications in work automation over the last few decades, revolutionizing the span of engineering and science techniques. Machine learning (ML) approaches have been widely investigated and implemented in antenna design in recent years because of their capacity to learn from measured or simulated antenna data via a training procedure and subsequently expedite the entire antenna design process [22]. When multiple parameters must be tuned, or complex structures must be designed, ML approaches have considerable advantages in decreasing significant computing times [23].

Once a dataset is obtained, it can be split into two parts: training and cross-validation, where the number of records in each depends on the total number of records present in the dataset. In the proposed antenna, 80 percent records are used for the training set and the other 20 percent are used for cross-validation sets.

In this paper, five algorithms have been used to make predictions: Decision Tree (DT) [24], Random Forest (RF) [25], XGBoost Regression [26], KNN [27], and Artificial Neural Network (ANN) [28, 29]. These algorithms are chosen because they can compute regression on nonlinear data. Since the desired output is in the form of numerical value, regression is the best possible method for making predictions. Python3 is used to implement these algorithms because it is easy to implement and has a large number of libraries available to support data preprocessing, machine learning algorithms, and visualization. Fig. 8 shows a flowchart for ML algorithm implementation. After studying the dataset, we divided the dataset into two parts. The first part contains an 80 percent training set and the second part contains 20 percent cross-validation set based on the recommendation in [30]. Then the training set is trained using a machine learning algorithm with various features and labels. After training and cross-validating the model, it can be used to predict the loss at resonating frequency for the desired inputs. Using ML, predictions are done in much less time with much less error margin than HFSS simulation results.

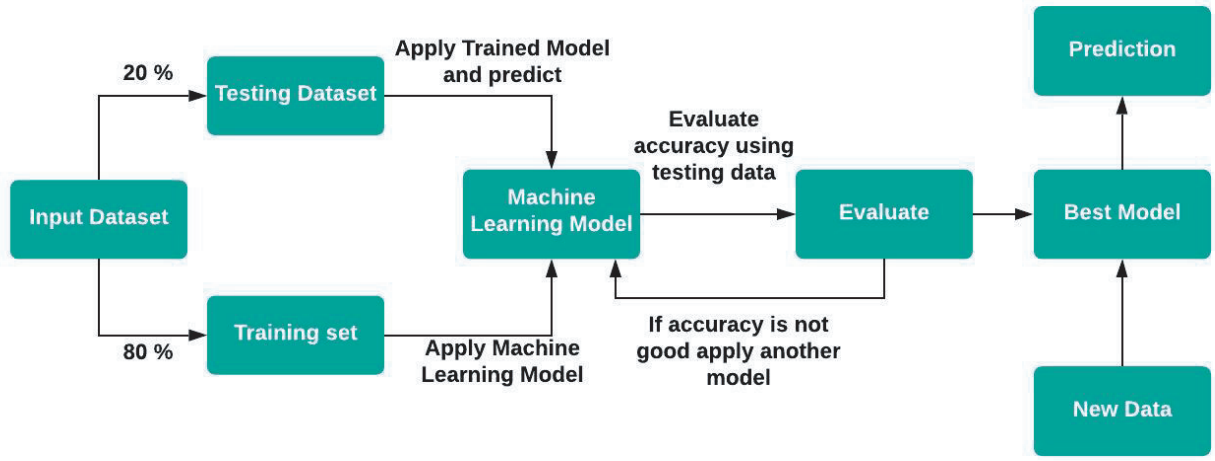

Figure 8. Machine learning algorithm implementation flowchart.

Table 3 summarizes the R-square scores and MSE value anticipated by several ML approaches. R-square score tells us how accurate our regression model is. It is the amount of variation in the output dependent attribute that can be predicted based on the input independent variable (s). Mean squared error (MSE) is measured as the average squared difference between predictions and actual observations. The R-square score and MSE value both are used to evaluate the performance of a regression-based machine learning model.

As shown in Table 3, KNN gives us the best prediction accuracy. Now, S_{11} is predicted with the assistance of KNN model. It gives us the minimum value for S_{11} equal to -35.77640827992235, where the width of L strip is 0.3 mm; horizontal length of L strip is -6.5 mm; and vertical length of L strip is

Table 3. Different models R-square score and mean squared error (mse).

	Model	R-square Score	MSE
1.	Decision Tree	0.919	0.933
2.	Random Forest (No Tuning)	0.961	0.509
3.	Random Forest (Hyper Parameter Tuning)	0.974	0.373
4.	XGBoost Regression	0.939	0.794
5.	K-Nearest Neighbor	0.978	0.290
6.	Artificial Neural Network	0.924	0.983

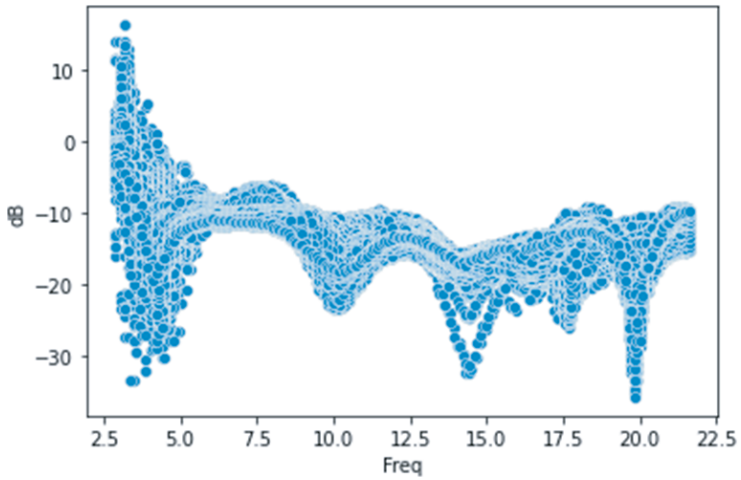

Figure 9. S_{11} prediction using KNN model.

Figure 10. Fabricated prototype of the proposed antenna.

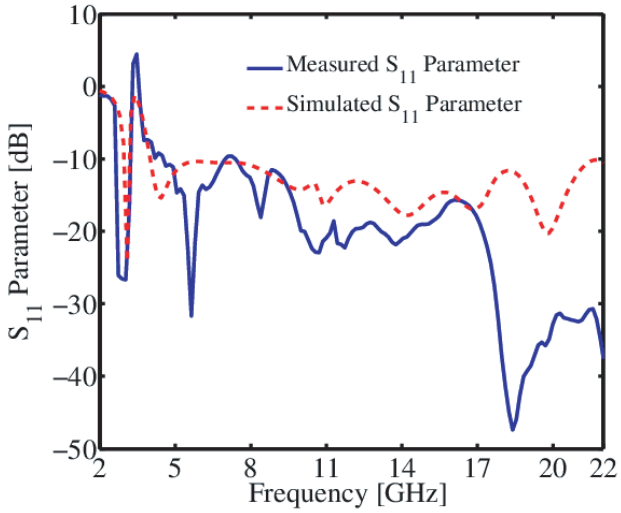

Figure 11. Simulated verses measured S-parameter of the proposed antenna.

10.0 mm at the frequency of 19.8235 GHz.

Figure 9 depicts the different S_{11} values predicted by KNN model for different frequency values. KNN performs better than the other algorithms because it is a non-parametric strategy that uses feature similarity to discover a predetermined number of training samples.

5. RESULTS AND DISCUSSION

The simulated prototype design of the antenna is fabricated using the PCB prototype machine as shown in Fig. 10. After the fabrication process, the results of the antenna are measured using the vector network analyzer.

The comparison of simulated and measured results of the antenna is shown in Fig. 11. From Fig. 11, it is observed that the results are in good correlation with each other. The little difference in the results is due to the fabrication connection losses.

The simulated radiation patterns of UWB band-notch antennas, in the E- and H-planes are shown in Fig. 12 at 3.3 GHz, 7.5 GHz, 13.2 GHz, and 20.1 GHz. However, for the notched frequency band at 3.3 GHz, the radiation pattern is unstable. For all the passband frequencies, the radiation pattern shows omnidirectional behavior.

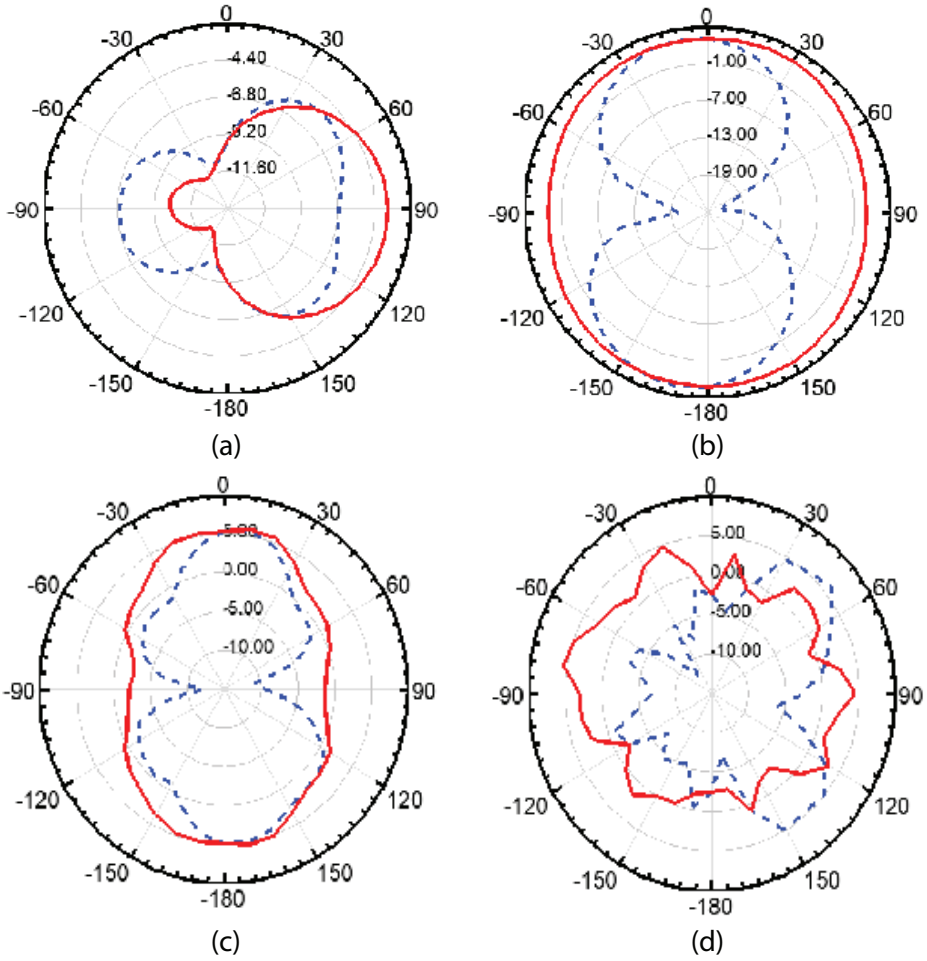

Figure 12. Radiation pattern at different frequencies for proposed antenna. (a) 3.3 GHz. (b) 7.5 GHz. (c) 13.2 GHz. (d) 20.1 GHz.

6. CONCLUSION

In this paper, a compact CPW fed monopole antenna with band notched feature is designed and optimized using ML algorithms. The optimized antenna design is also fabricated and tested, which confirms that its frequency range lies between 2.9 and 21.6 GHz. In the operating frequency band, the stable radiation feature makes it suitable for UWB applications. Five distinct machine learning algorithms are utilized to predict the optimal values of design parameters: Decision Tree, Random Forest, XGBoost Regression, K-Nearest Neighbor, and Artificial Neural Network. In this investigation, K-Nearest Neighbor (KNN) provides more accurate predictions than others. In conclusion, antenna optimization is more effective with ML algorithms than traditional EM simulators.

REFERENCES

1. Revision of Part 15 of the Commission's rules regarding ultra-wide-band transmission systems First report and order FCC 02.V48, Federal Communications Commission, Washington, DC, 2002.
2. Chang, K., H. Kim, and Y. J. Yoon, "Ultra-wideband antenna with improved gain characteristics," *IET Microwaves, Antennas Propagation*, Vol. 2, No. 5, 512–517, August 2008.
3. Malekpour, H. and S. Jam, "Enhanced bandwidth of shorted patch antennas using folded-patch techniques," *IEEE Antenna and Wireless Propagation Letters*, 198–201, 2013.
4. Kim, G. H. and T. Y. Yun, "Compact ultrawideband monopole antenna with an inverted-L-shaped coupled strip," *IEEE Antenna and Wireless Propagation Letters*, Vol. 12, 1291–1294, 2013.
5. Chen, S. J., T. Kaufmann, R. Shepherd, B. Chivers, B. Weng, A. Vassallo, et al., "A compact highly efficient and flexible polymer ultra-wideband antenna," *IEEE Antennas and Wireless Propagation Letters*, Vol. 14, 1207–1210, December 2015.
6. Ranjan, P. and H. Gupta, "Investigation of dual-band rectangular dielectric resonator antenna with DGS for wireless applications," *2021 IEEE Bombay Section Signature Conference (IBSSC)*, 1–4, 2021.
7. Gautam, A. K., S. Yadav, and B. K. Kanaujia, "A CPW fed compact UWB microstrip antenna," *IEEE Antennas and Wireless Propagation Letters*, Vol. 12, 151–154, 2013.
8. Gao, P., S. He, X. Wei, Z. Xu, N. Wang, and Y. Zheng, "Compact printed UWB diversity slot antenna with 5.5-GHz band-notched characteristics," *IEEE Antennas and Wireless Propagation Letters*, Vol. 13, 376–379, 2014.
9. Zhu, F., S. Gao, A. T. S. Ho, R. A. Abd-Alhameed, C. H. See, J. Li, et al., "Miniaturized tapered slot antenna with signal rejection in 5–6 GHz band using a balun," *IEEE Antennas and Wireless Propagation Letters*, Vol. 11, 507–510, 2012.
10. Gautam, A. K., Indu, and B. K. Kanaujia, "Dual band-notched rectangular monopole antenna for ultra wideband application," *Microwave and Optical Technology Letters*, 12, December 2013.
11. Rajeshkumar, V. and S. Raghavan, "Bandwidth enhanced compact fractal antenna for UWB application with 5–6 GHz band rejection," *Microwave and Optical Technology Letters*, Vol. 57, 607–613, 2015.
12. Devi, M., A. K. Gautam, and B. K. Kanaujia, "A compact ultra wideband antenna with triple band-notch characteristics," *International Journal of Microwave and Wireless Technologies*, 2015.
13. Nguyen, D. T., D. H. Lee, and H. C. Park, "Very compact printed triple band-notched UWB antenna with quarter-wavelength slots," *IEEE Antennas and Wireless Propagation Letters*, 411–414, December 2012.
14. Wu, Q., Y. Cao, H. Wang, and W. Hong, "Machine-learning-assisted optimization and its application to antenna designs: Opportunities and challenges," *China Communications*, Vol. 17, No. 4, 152–164, 2020.
15. Wu, Q., W. Chen, C. Yu, H. Wang, and W. Hong, "Multilayer machine learning-assisted optimization-based robust design and its applications to antennas and array," *IEEE Transactions on Antennas and Propagation*, Vol. 69, No. 9, 6052–6057, September 2021.

16. Shi, M., L. Cui, H. Liu, M. Lv, and X. Sun, "A new UWB antenna with band-notched characteristics," *Progress In Electromagnetics Research M*, Vol. 74, 201–209, 2018.
17. Saed, M. and R. Yadla, "Microstrip-fed low profile and compact dielectric resonator antennas," *Progress In Electromagnetics Research*, Vol. 56, 151–162, 2006.
18. Tang, M. C., H. Wang, T. Deng, and R. W. Ziolkowski, "Compact planar ultrawideband antennas with continuously tunable, independent band-notched filters," *IEEE Transactions on Antennas and Propagation*, 3292–3301, 2016.
19. Rezaeieh, S. A. and M. Abbak, "A novel compact antenna enhanced with variable notches," *Microwave and Optical Technology Letters*, 946–949, 2012.
20. Sarkar, M., S. Dwari, and A. Daniel, "Compact printed monopole antenna for ultra-wideband application with dual bandnotched characterstic," *Microwave and Optical Technology Letters*, 946–949, 2013.
21. Rahman, M., M. Nageshvara Jahromi, S. S. Mirjavadi, and A. M. Hamouda, "Compact UWB band-notched antenna with integrated bluetooth for personal wireless communication and UWB applications," *Electronics MDPI*, 2019.
22. Sharma, Y., H. H. Zhang, and H. Xin, "Machine learning techniques for optimizing design of double T-shaped monopole antenna," *IEEE Transactions on Antennas and Propagation*, Vol. 68, No. 7, 5658–5663, 2020.
23. El Misilmani, Hilal M., TarekNaous, and Salwa K. Al Khatib, "A review on the design and optimization of antennas using machine learning algorithms and techniques," *International Journal of RF and Microwave Computer-Aided Engineering*, Vol. 30, No. 10, e22356, 2020.
24. Chauhan, N. S., Decision Tree Algorithm — Explained, towards data science, [Online], Available: https://towardsdatascience.com/decision-tree-algorithm-explained-83beb6e78ef4.
25. Breiman, L., "Random forests," *Machine Learning*, Vol. 45, No. 1, 5–32, 2001.
26. Vishal MordeXGBoost Algorithm — Explained, towards data science, [Online], Available: https://towardsdatascience.com/https-medium-com-vishalmorde-xgboost-algorithm-long-she-may-rein-edd9f99be63d.
27. Cui, L., Y. Zhang, R. Zhang, and Q. H. Liu, "A modified efficient KNN method for antenna optimization and design," *IEEE Transactions on Antennas and Propagation*, Vol. 68, No. 10, 6858–6866, October 2020.
28. Sallam, T., A. B. Abdel-Rahman, M. Alghoniemy, Z. Kawasaki, and T. Ushio, "A neural-network-based beamformer for phased array weather radar," *IEEE Trans. Geosci. Remote Sens.*, Vol. 54, No. 9, 5095–5104, September 2016.
29. Wang, J. R., W. J. Liu, and M. S. Tong, "An artificial neural network based design of triple-band microstrip patch antenna for WLAN applications," *2020 IEEE MTT-S International Conference on Numerical Electromagnetic and Multiphysics Modeling and Optimization (NEMO)*, 1–4, 2020.
30. Training and Test Sets: Splitting Data. Machine Learning Crash Course, [Online], Available: https://developers.google.com/machine-learning/crash-course/training-and-test-sets/splitting-data.